ORIGINAL ARTICLE

Study on the mechanism of roof collapse and leakage of horizontal cavern in thinly bedded salt rocks

Zhixin Zhang[1,2] · Deyi Jiang[1,2] · Wei Liu[1,2] · Jie Chen[1,2] · Erbing Li[3] · Jinyang Fan[1,2] · Kainan Xie[1,2]

Abstract

In the thinly bedded salt formations, due to the limited thickness of the salt strata along with the fast upward dissolution, the collapse of the non-salt roof of the cavern often occurs, leading to the leakage of brine and instability of the cavern as well as other undesirable geological consequences. To investigate the gypsum-salt interbedded roof collapse, the failure mechanism and the control methods of Dainan siltstone, which is the indirect roof of the horizontal salt caverns in Zhaoji Salt Mine, were thoroughly investigated. Through the drilled cores from this mine, a series of contrast tests such as SEM, EDS, XRD, soaking, and nuclear magnetic properties were carried out to study the physical properties of the salt layer and non-salt layer of the cavern roof and to determine the cavern roof collapse and leakage mechanism. Using the Comsol software, the model of a horizontal cavern roof leakage was established, and the leakage range and leakage of brine at different time were analyzed, as well as the safety problems caused by it. Finally, some suggestions have been provided for the leakage control of the cavern roof in bedded salt cavern.

Introduction

In recent years, the construction and operation of hydrocarbon oil and gas underground storage facilities have developed rapidly both domestically and abroad (Lux 2009; Yang et al. 2015; Liu et al. 2016a). As a kind of special geological material with low permeability (Cosenza et al. 2009; Liu et al. 2016b), low porosity (Cuevas 1997), excellent plastic ability (Chen et al. 2016; Wu et al. 2018) and damaged self-healing ability (Houben et al. 2013), salt rock is reputed to be an excellent option to construct oil and gas storage caverns (Zhang et al. 2017), waste disposal (Shi et al. 2015) and compressed air energy storage (Djizanne et al. 2014; Zhang et al. 2015). At the same time, the financial charges related

to water-soluble cavern are convenient, and the operation of this kind of storage caverns in the later stage is safe and stable (Johnson and Seni 2001), which makes the oil and gas storage in salt caverns better than other types of storage facilities and now appears to be an desirable choice for oil and gas storage in many countries (Yang et al. 2013). The horizontal cavern has better geological adaptability regarding storage space in the bedded salt rocks (Xing et al. 2015). And because of its rapid rate of construction, large capacity and good economy, it has become a suitable method to extract brine or to create caverns in bedded salt rocks, especially in the case of thinly bedded salt formations (Liu et al. 2018). In the Middle East of China, there are a large number of thinly bedded salt rocks, in which horizontal caverns are often used for brine withdrawal. With the large demand of oil and gas storage in central and eastern China these years, more and more scholars have proposed to use horizontal cavern for energy storage (Xing et al. 2015; Liu et al. 2018).

The stability and tightness (Zhang et al. 2014; Chen et al. 2018) of the cavern are key factors to determine whether the brine extraction or caverns construction can develop smoothly, or ensure the following storage of oil and gas be feasible. However, due to the existence of factors such as the limited thickness of salt strata and difficulty of solution

✉ Wei Liu
  whrsmliuwei@126.com

1   State Key Laboratory of Coal Mine Disaster Dynamics
    and Control, Chongqing University, Chongqing 400044,
    China

2   College of Resources and Environmental Sciences,
    Chongqing University, Chongqing 400044, China

3   Engineering Institute of Engineering Crops, the Army
    Engineering University of PLA, Nanjing 210000, China

control in salt rock, there are many technical challenges for constructing a safe and stable cavern in thinly bedded salt rocks (Li et al. 2012; Shi et al. 2018). If the solution control is not correct, the cavern formed later may be in the risk of brine leakage, roof instability, etc. If these problems are not found and solved in time, there will be a huge potential risk during oil and gas storage. Therefore, to promote safety during cavern construction and operation, it is necessary to pay attention to the development process of the cavern roof and make reasonable investigations on its leakage mechanism and control measures and so on.

Domestic and foreign research on salt cavern stability and sealing mostly focused on single-well cavern. In the early 1980s, using the finite element program, Preece and Foley (1983, 1984) analyzed the volume contraction of the Weeks Island gas storage cavern caused by salt creep deformation, and predicted the volume loss after operating 50 years. Ma et al. (2015) analyzed the cavern stability as gas storage based on new partitions of the surrounding rock. In case of horizontal wells, Yang et al. (2016) have conducted numerical simulation on the stability and roof safety state of the salt gas storage in Yunying Salt mine, but the erosion and softening of the roof cap rock is out of consideration. Liu et al. (2018) conducted a comprehensive feasibility study on two-well-horizontal caverns for natural gas storage in China's thinly bedded salt rocks. It can be seen that current research on the stability and operations of the horizontal caverns in salt rock is all based on the premise that the horizontal cavern has a regular shape, sufficient thickness of roof salt layer, and impermeable roof cap rock. However, these conditions are too idealistic, and the actual engineering might differ much.

China has an enormous reserve of salt mines and a long history of water-solution salt mining. Most of the salt mines in China are the lacustrine sedimentary type, thus are bedded structure. The salt layers are numerous and thin, and the total salt-bearing strata are also very limited (usually less than 200 m). Thus, two wells are largely used for brine withdrawn, and horizontal caverns are usually created. The upward dissolution rate of salt rock is much larger than the rates in other directions. As a result, the roof solution of the salt cavern is rather hard to control. In the case of thinly salt beds and permeable cap rock, both roof failure and brine leakage may occur at the same time. In this study, the background is the horizontal cavern water solution in one salt mine in Jiangsu Province, eastern China. As the failure of roof solution control, brine leakage appears. To investigate the reason of brine leakage and the mechanism of roof failure, the geological exploration data of this salt mine were analyzed, and the core samples of the salt cavern roof and the interlayer of the mine were studied. The mechanism of cavern leakage along with the roof failure developing process was determined. Numerical simulations were also conducted to reveal the brine leakage in the siltstone roof. In the end, effective measures and suggestions to lessen or control these problems were also discussed.

Geological features and leakage status

Structure and formation of salt mine area

The salt mine is located in the northeast of Hongze sag of Subei basin, called Zhaoji sub-sag (Fig. 1a). Seismic exploration and drilling data show that it is a typical south–north super-loop fault basin, and generally, fan shaped to the northeast. According to basement fluctuation, deposit and fracture characteristics, from SE to NW, it can be divided into broken order zone, deep concave belt, and slope zone. The deep concave belt is the depositional center of Zhaoji sub-sag, which is a good region for salt deposit. The lithology and lithofacies of the slope zone have undergone dramatic changes, mainly composed of gypsum fractal facies. The internal structure of Zhaoji is relatively simple and is characterized by the fact that fault is not developed, and the boundary fault of SN and NE can be seen within the four sides of the depression, and a subgrade fault is found in the slope zone.

Basic geological features and leakage status

Salt-bearing system occurs in paleogene in four sections of Funing formation (E_1f_4), which can be further divided into five lithologic sections: gypsum bed over upper salt bed section, upper salt bed section, midst fresh section, lower salt bed section, and gypsum bed below lower salt bed section, as shown in Fig. 1b and Table 1.

The lower salt bed section and the upper salt bed section are the main salt deposits. The upper salt layer roof is buried at a depth of 1350–2010 m, and the direct roof of the salt ore body is the top layer of E_1f_4, with a thickness of 4–50 m. The floor is buried at a depth of 1450–2176 m, which is the desalination layer between the upper salt subsection and the lower salt subsection in E_1f_4, with a thickness of 45–82 m. The sedimentary structure of the salt-bearing strata is stable, and the lithologic changes are small. The thickness of this stratum is 118.60–142.94 m, among which, the salt rock thickness reaches 103.60–130.33 m, making it the main exploration and development layer of the salt rock body. The interlayer is composed of gray calcareous mirabilite mudstone, gypsum mudstone, and mudstone, with a thickness of 0.2–1.8 m. The salt content of the upper salt subsection is comprised between 87.4 and 91.18%, and its main component is gray salt rock, mixed with a thin layer of brown-gray sandy mudstone and glauberite rock, and a small amount of impurity clay minerals, calcite, and dolomite.
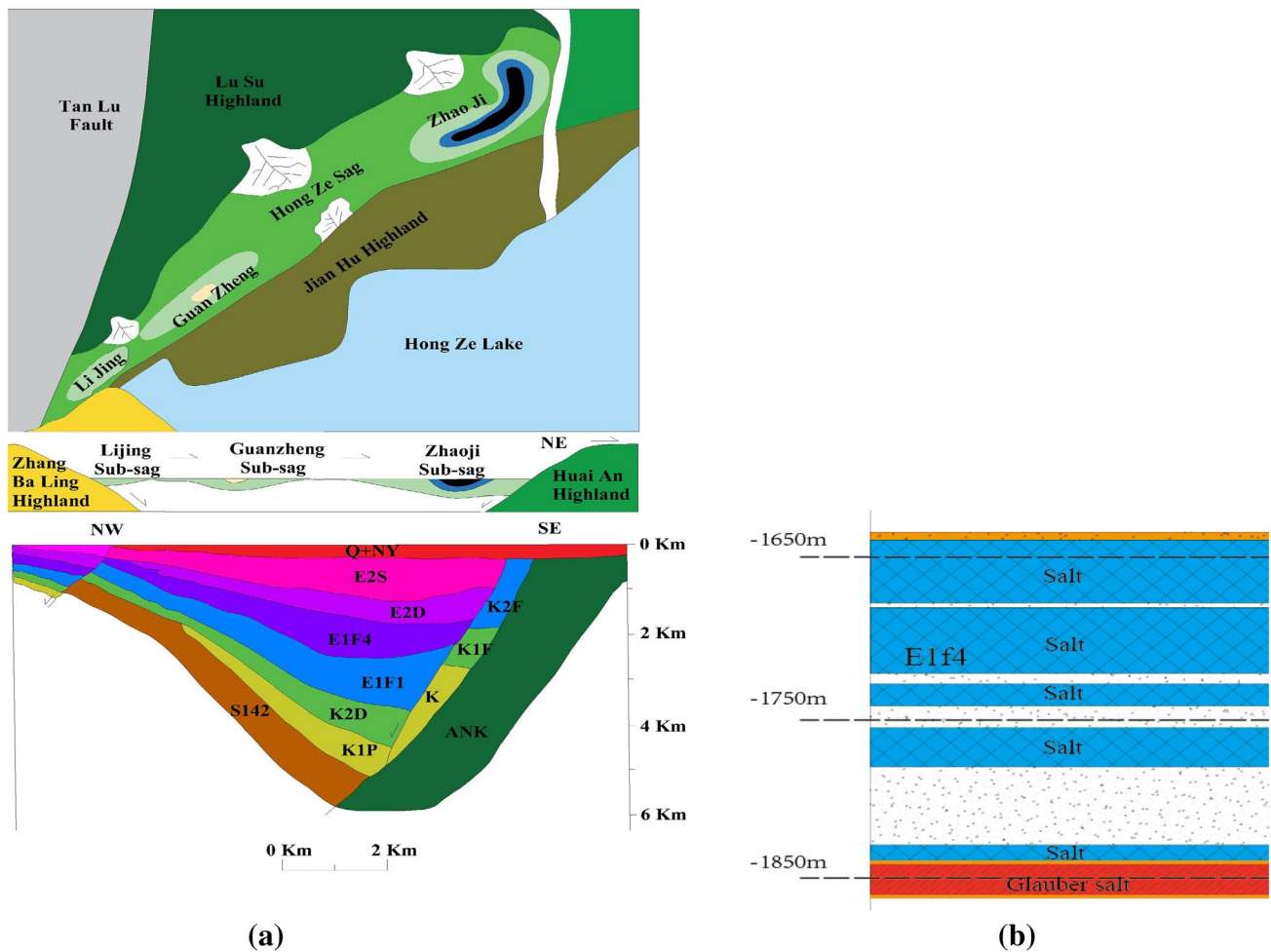
Fig. 1 Geological and geo-strata information: **a** schematic diagram of Zhaoji sug-sag geological structure in Hongze sag and **b** distribution schematic of salt-bearing strata

Table 1 Characteristic table of Zhaoji sub-sag

Group	Paragraph	Section	Thickness (m)	Lithological characters
Funing (E_1f)	Four (E_1f_4)	Gypsum bed over upper salt bed	3.56–10.50	Gray and gray-black anhydrite and argillaceous gypsum
		Upper salt bed	60.00–150.00	Gray salt rock, mixed with anhydrite and glauberite rock
		Midst fresh	71.50–115.00	Calcareous mudstone and mudstone
		Lower salt bed	> 12.80–104.72	Rock salt, anhydrite, and glauberite rock
		Gypsum bed below lower salt bed	> 322.00	Interaction layer of anhydrite and mudstone; gray mudstone, dolomitic mudstone and carbonate rock

As shown in Fig. 2, the horizontal cavern was buried at a depth of 1600–1720 m and was located between the gypsum bed over upper salt bed section and the upper salt bed section. The main composition includes the lime-white salt rock, which is mixed with argillaceous gypsum rock interlayer. The direct roof of the horizontal cavern consists of gypsum layers with a thickness of about 5 m, above it is the Dainan siltstone (E_2d) with a thickness of over 80 m. Above

Dainan siltstone is thick mudstone and silt mudstone, with a thickness over 800 m, which separates the Dainan siltstone with the overly ground water-bearing strata. It also found the Dainan siltstone stratum contains almost no initial water by drilling data. Two wells, SY16 and SY21, were connected using docking connection technology of horizontal wells at 1715 m underground, where SY16 Well was a vertical well and SY21 Well was an inclined well. There is no obvious

Fig. 2 Probable cause of brine roof failure and brine leakage: after the gypsum layer was softened and collapsed, the high-pressure brine penetrated the Dainan siltstone and caused the leakage of brine
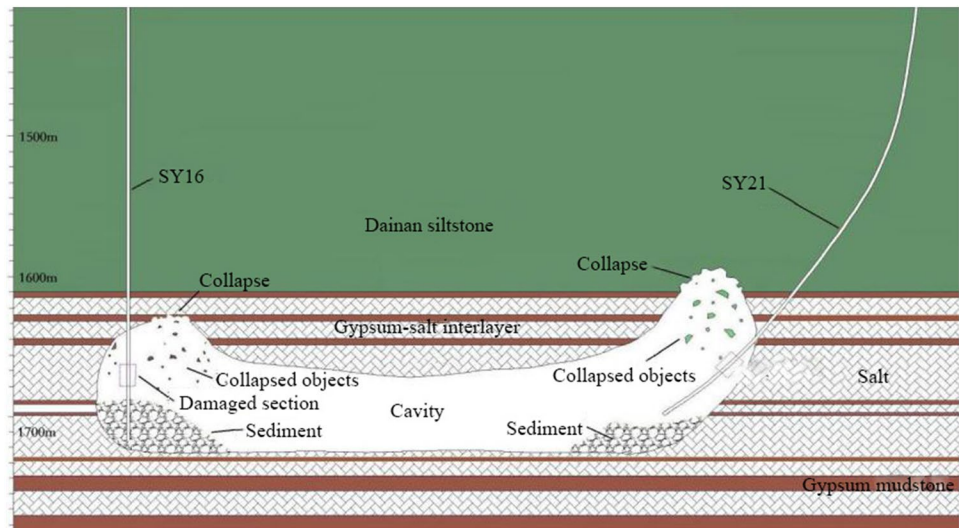
fault around the assigned region of the salt mining stratum, including roof and floor strata. And the contacting roof and floor strata are dense and free with underground water. So the initial geological data indicate the sealing properties of the salt-bearing strata are good. Generally, injected fresh water balances with withdrawn brine (volume ratio: brine: fresh water ≈ 0.96). However, in this horizontal cavern (SY16 and SY21), it was found that over thousand cubic meters of brine was missing within 1 year during the production from 2015 to 2016.

Consider that the roof of the salt cavern is intersected by gypsum-salt layers, vulnerable to water erosion. If no effective upper solution control measures are taken in the field operation, it may be exposed due to the rapid dissolution of the cavern, and then the gypsum layers collapse under the soaking of high-pressure brine. Above the intersected gypsum-salt layers, there is the Dainan siltstone layer. If the permeability of the Dainan siltstone rock is strong, after the gypsum layers are eroded and collapse, high-pressure brine would be in contact with the siltstone layer and penetrate into it, which may be the main cause of leakage of brine (Fig. 2). Based on the deduction above, SEM, EDS and XRD experiments of the cavern roof were designed and carried out, and the failure mechanism of the roof was further investigated based on the analysis of nuclear magnetism, softening soaking and water absorption characteristics of roof layers.

Physical experiment and result analysis

To reveal the mechanism of cavern leakage, a series of studies were carried out on the gypsum strata and the Dainan siltstone in the roof of the salt mine, which mainly used the X-ray diffraction (XRD) and scanning electron microscope

(SEM) and energy-dispersive spectrometer (EDS) to analyze the microstructure and components of the drilling cores. The core samples were obtained from SY21 well and SY16 well, buried at a depth between 1670 m and 1820 m, and the whole work was carried out in these sections. Finally, representative cores were selected for the further experimental study.

SEM and XRD experiments

According to the samples' condition, we carried out the SEM experiment to study the difference of microstructure on the core surface, and a preliminary analysis of the sample composition was obtained by EDS spectroscopy. Furthermore, the composition and structure of impurities in the sample were obtained by XRD experiment. As the sample was processed, representative samples were selected and used as the experimental specimens. Three typical core samples of clay siltstone (Dainan siltstone), gypsum mudstone and gray rock salt were selected and are shown in Fig. 3.

Analysis of experimental results

SEM and EDS experimental results

For the sample prepared, the SEM results of gray salt rock are shown in Fig. 4. It can be found that there are two states in the microscopic structure of the salt rock in the sample: a square sodium chloride crystal and a cluster of sodium chloride crystals. The junction of the two has a pore size of 20–30 μm, which provides a channel for the upward penetration of the brine.

The EDS survey results of clay siltstone and gypsum mudstone are shown in Fig. 5, both the samples had lots of micropores and fissures, with a low density. As the results

Fig. 3 Three typical core samples ($\varphi = 100$ mm)

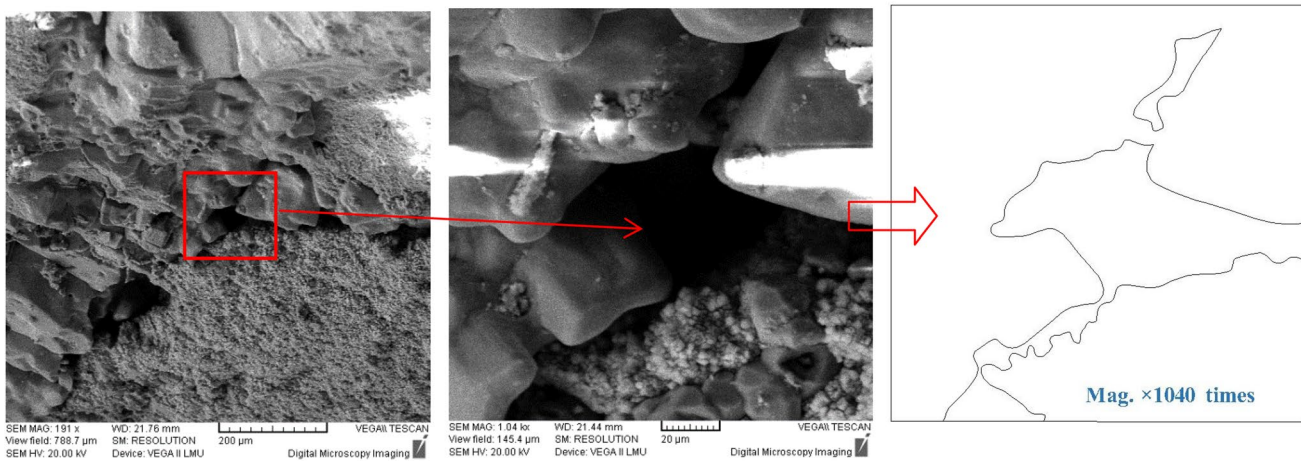**(a)** Clay siltstone   **(b)** Gypsum mudstone   **(c)** Grey rock salt

Fig. 4 SEM results of gray salt rock

show, the pore size of the clay siltstone sample is between 10 and 100 μm, while its main components are montmorillonite minerals, quartz, tremolite, zircon and so on. The pore size of the gypsum mudstone sample is between 10 and 60 μm, and the main components of it are calcium sulfate, quartz, clay minerals and so on.

As the SEM and EDS results of three typical lithologies of roof interaction layer showed, developed micropore and fissure will provide channels for the seepage of high-pressure brine, will reduce the effective stress within the rock mass, and will also cause the softening of the internal gypsum along with the expansion of clay minerals due to water absorption. These combined effects will accentuate the destruction and failure of gypsum rock formations.

XRD results of roof rock layers

The XRD test is used to determine the compositions of the roof rock layers, after having figured out its microscopic characteristics and formation mechanism. Table 2 shows the composition analysis results of Samples 1–6, from which it can be seen that part of the roof rock layers contains a large number of clay mineral or gypsum. These substances are prone to expansion or being softened due to water, affecting the mechanical strength and stability of roof rock.

The direct roof of the salt cavern is gypsum mudstone, and its main compositions in the sample are gypsum (50%), quartz (20%), with very little trace of clay minerals. With mining operations, the cavern height increases, and gypsum strata in the roof are gradually exposed, internal stress is released, and the stratification gradually appears, creating cracks or fractures at the layer. Gypsum is softened by water, and the high-pressure brine may penetrate the gypsum layer or the halite fissures, causing further damage and softening of the gypsum strata, resulting in collapse. After the roof of gypsum mudstone was softened and completely collapsed, the brine in the cavern came in direct contact with the Dainan siltstone. To better understand the leakage mechanism of the roof, we then studied the water absorption and conductivity properties of the gypsum mudstone and clay siltstone.
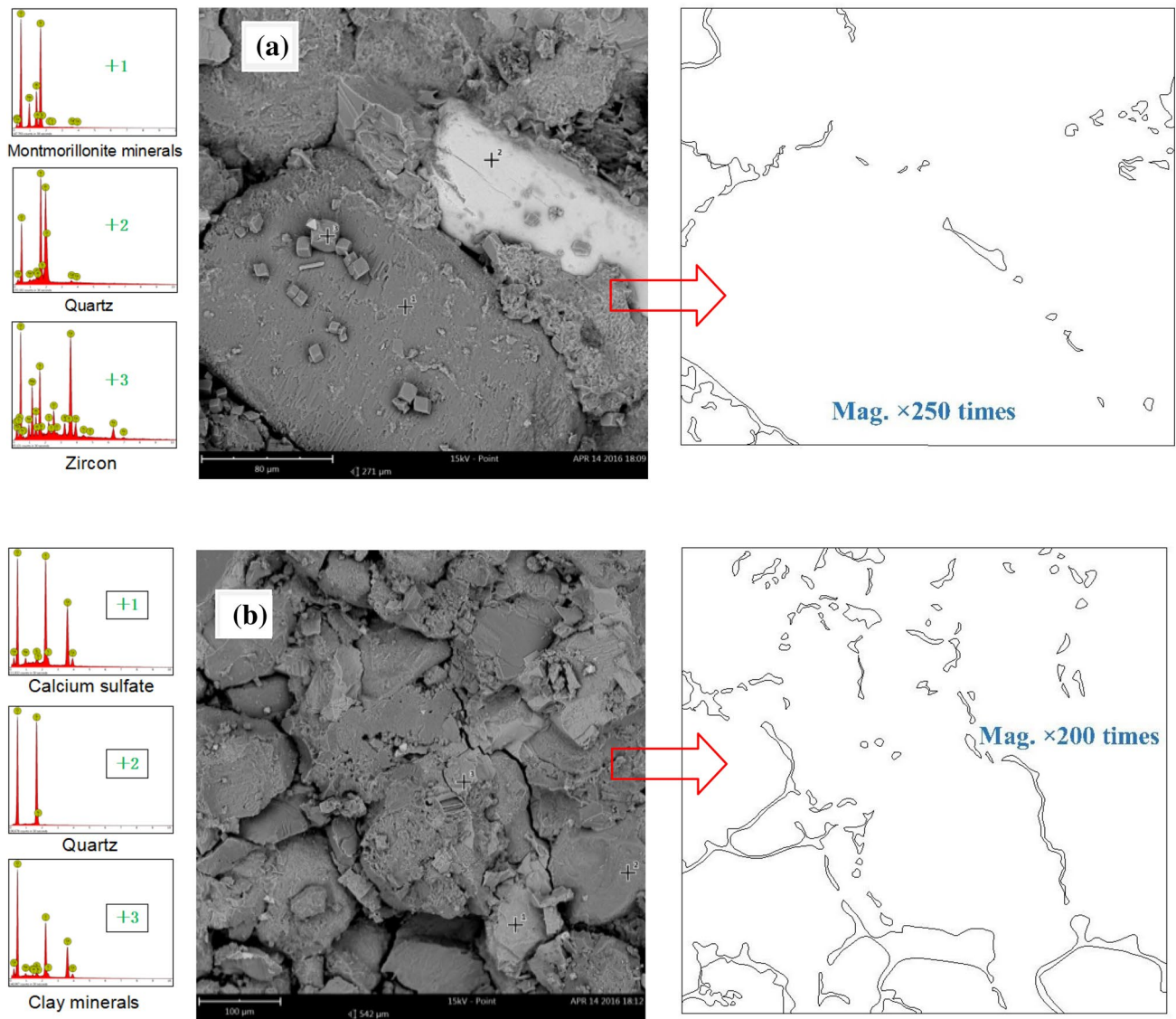
Fig. 5 EDS diagram of clay siltstone (**a**) and gypsum mudstone (**b**)

Table 2 Composition analysis results of Samples 1–6

Number	Rock types	Quartz (%)	Illite (%)	Gypsum (%)	Feldspar (%)	Others (%)
1	Clay siltstone	40	15	–	25	20
2	Clay siltstone	30	30	5	25	10
3	Clay siltstone	50	4	–	32	14
4	Mudstone	20	43	4	16	17
5	Mudstone	29	18	3	24	26
6	Gypsum mudstone	20	15	50	15	–

Water absorption and conductivity of roof rock

Soak experiment

In the process of salt cavern development, the upward dissolution is generally faster than that of the sides about twice as much as the rate of side solution (Liu et al. 2016c). Salt rock will be dissolved rapidly at the roof layer if there are no effective protections for upward dissolution. Petro-physical analysis has revealed that the main components of the direct cavern roof are gypsum mudstone. Under the soaking of high-pressure brine, it would absorb water and expand, and both physical and chemical reactions would occur in this process (Bekendam et al. 2000; Shi et al. 2009), leading to an obvious softening and peeling of the rock mass. To study the water absorption characteristics of roof rock layer and its overlying layer, water soaking experiments were carried out on gypsum mudstone and Dainan siltstone under a pressure of 19 MPa (Equaling the maximum in situ brine pressure in cavern). The experimental devices are shown in Fig. 6, as well as some samples of the gypsum mudstone and Dainan siltstone, where Sample 1 is gypsum mudstone, and Samples 4 and 7 are Dainan siltstone. After a full drying of the samples, the soaking experiment is carried out at 19 MPa in the distilled water.

During the experiment, the sample quality was measured every 0.5 h, and the change of water content in sample was detected using nuclear magnetic resonance (NMR), which gave the water absorption of sample and then the water absorption rate of the sample was calculated. Two hours later, the water absorption process of sample was basically completed, and the relevant data of the experiment during 4 h were recorded, as shown in Table 3.

The changes in the quality and water absorption rate of the samples were analyzed. As shown in Fig. 7, there was a significant increase in sample quality and water absorption rate within the beginning 0.5 h. It showed that, during the early stage of the experiment, completely dry gypsum mudstone and Dainan siltstone have strong water absorption in a high-pressure immersion environment. And then the sample quality began to decline, but there was still a small increase in water absorption rate even though water absorption process was slowed down. From previous experiments,

Fig. 6 Schematic diagram of soak test devices and samples of Dainan siltstone and gypsum interlayer ($\varphi = 25$ mm)
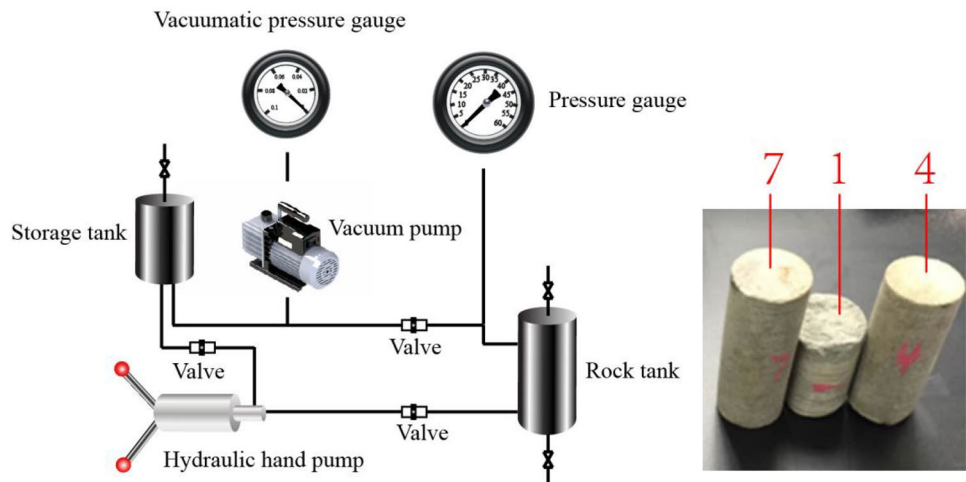
Table 3 Changes in quality and water absorption of samples with immersion time

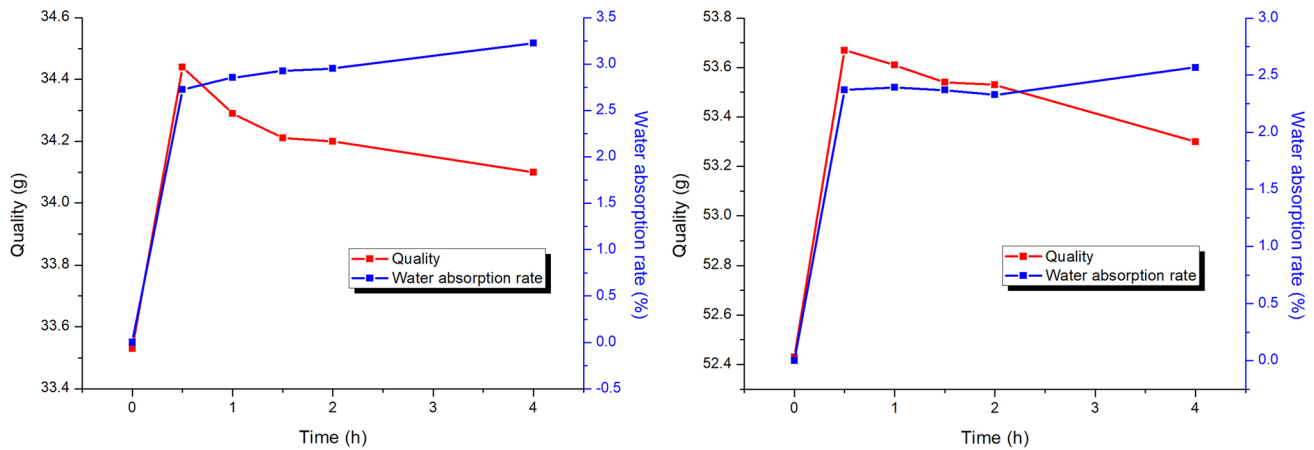| Immersion time (h)	Sample 1		Sample 4		Sample 7	
	Quality (g)	water absorption (g)	Quality (g)	water absorption (g)	Quality (g)	water absorption (g)
0	33.53	0	52.43	0	57.67	0
0.5	34.44	0.91373	53.67	1.24357	59.11	1.44273
1.0	34.29	0.95639	53.61	1.25461	59.09	1.42182
1.5	34.21	0.98107	53.54	1.24204	59.06	1.37675
2.0	34.20	0.98932	53.53	1.22027	58.99	1.43241
4.0	34.1	1.08191	53.30	1.34623	58.78	1.55943

Fig. 7 Change of quality and water absorption rate of Samples 1 and 4 (left image is Sample 1, and the right image is Sample 4)

we could see that for the samples containing clay minerals, which swelled after absorbing water, would cause the peeling of the surface minerals and softening of the matrix. Meanwhile, as the internal part was filled with water, the expansion may have also blocked the pores and slowed down the absorption of water. The reason why the total quality was reduced after having absorbed the water is that minerals, such as gypsum and illite in the sample, were removed from the sample after having been softened and expanded during the soaking experiment.

At the same time, it can be seen that the quality reduction of gypsum mudstone samples is larger than that of the Dainan siltstone, and the water absorption rate is greater than that of the Dainan siltstone. The underlying reason is that the gypsum content of gypsum mudstone is much higher than that of Dainan siltstone and complicated physical and chemical reactions occurred after gypsum had absorbed water and then gradually went through softening and peeling, which is also the main reason for the decrease in sample quality. The experiment confirmed that gypsum mudstone would be softened and peeled off after soaking in high-pressure brine, resulting in the collapse of the roof layer. To explore the internal microscopic characteristics of Dainan siltstone and gypsum mudstone, a nuclear magnetic experiment has been prepared.

Nuclear magnetic experiment

As shown in Fig. 8, the nuclear magnetic analysis system was used to conduct a nuclear magnetic analysis of the roof layer. To obtain the correlation coefficient of porosity and permeability of the roof core sample, two groups of experiments were set up, namely group Dainan siltstone (Sample 12) and group gypsum mudstone (Sample 13).

Before the nuclear magnetic test, the dry sample was placed in the vacuum pressure saturation device. Then the device was pumped into the vacuum, and distilled water was injected, and the pressure was set at to 19 MPa. Finally, the core was fully saturated, and 24 h later, it was placed into the nuclear magnetic machine for detection. Figure 9 shows the imaging profile of group Dainan siltstone under nuclear magnetic detection after 24 h immersion, in which the white
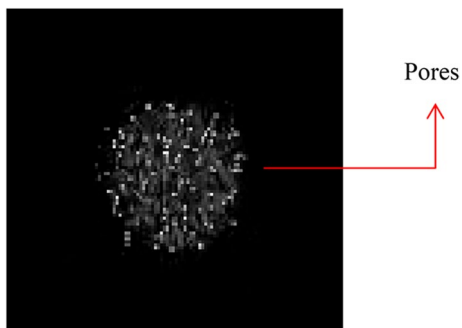
Fig. 8 The Nuclear magnetic analysis system

Fig. 9 The imaging profile of Dainan siltstone ($\varphi = 25$ mm) after 24 h immersion

parts represent water in the sample pores. It can be seen from the figure that the Dainan siltstone is a typical porous medium, the matrix of which is filled with water in a high-pressure environment. The result has proved that there was a high probability so that the brine would penetrate into the Dainan siltstone layer after the roof of gypsum mudstone had corroded and completely collapsed.

The nuclear magnetic resonance detection results are shown in Table 4. And as we can see, the porosity of Dainan siltstone sample is 9.55%, and the value of gypsum

mudstone is also relatively close (9.47%). However, the permeability difference between the two is relatively large. The gypsum mudstone has a permeability of 0.155×10^{-15} m^2, while the permeability of Dainan siltstone is as high as 4.82×10^{-15} m^2, which is about 31 times than that of the former. That is to say, the permeability of the gypsum mudstone layer is much lower compared to Dainan siltstone. With the exposure of the roof of the cavern, stratification of gypsum mudstone would easily occur, which would actually increase the channel for the brine leakage. When the siltstone layer is exposed, its relatively high permeability provides a good condition for the brine penetration. This is the reason for the loss of brine in cavern.

Roof leakage mechanism

The water absorption and nuclear magnetic experiments have revealed the evolution characteristics of the roof layer under the action of brine soaking, which is gradual softening, stripping and collapsing. Thus, the evolution process of the cavern and roof can be understood as shown in Fig. 10.

(a) In the early stage, with the continuous injection of fresh water, cavern expanded and the upper dissolution rate was obviously faster than that of the lateral sides.

Table 4 Results of NMR examination

Core type	Pre-saturation quality (g)	Saturation quality (g)	Quality increasing (g)	Porosity (%)	Free fluid saturation (%)	Permeability (10^{-15} m^2)
Dainan siltstone	56.19	58.71	2.52	9.55	37.571	4.820
Gypsum mudstone	32.71	34.09	1.78	9.47	9.866	0.155

(a) The early　　　　　(b) The middle　　　　　(c) The late

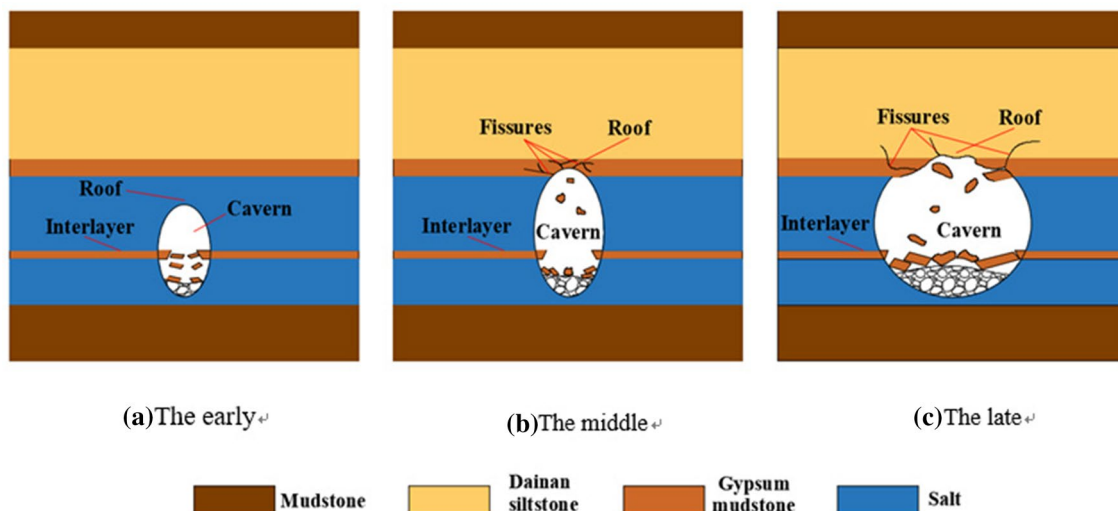Mudstone　　Dainan siltstone　　Gypsum mudstone　　Salt

Fig. 10 Schematic diagram of cavern and roof evolution

Before being in contact with the gypsum mudstone layer, the cavern shape was approximately elliptic.

(b) In the middle stage, cavern enlarged and the roof of the cavern was developing continuously, gypsum mudstone layer was gradually exposed to brine and the soluble contents dissolved, stratification was gradually opening, and the rock matrix was softened and dropped down. At the same time, the swelling of the clay minerals in the gypsum mudstone layer caused the development of internal fissures, which increased the speed of brine erosion and internal structure destruction.

(c) In the late stage, the gypsum mudstone was collapsed completely. The brine then contacted in direct with the Dainan siltstone, which meant that the Dainan siltstone layer became the direct roof of the cavern. And as a result, brine would penetrate into the siltstone layer. And at this point, the cavern leakage would occur.

It is important to emphasize that, once the protective salt layer (the salt rock remained at the roof to protect the cavern stability and tightness) at the roof of the cavern is destroyed, the brine will then contacted with the permeable stratum. Then it is very difficult to continue the process of developing the cavern. In addition, the stability of the cavern roof will also be greatly impacted. For the gypsum mudstone strata, the bearing capacity is basically lost after immersion. And for the siltstone layer, even if the roof is stable for a short time, the decrease in the safety factor caused by the penetration of the brine might be also very significant. As shown in Fig. 11, after the brine penetrates into the siltstone roof, the pore water pressure induces the effective stress to decrease, which will cause the downward moving of the shear failure envelope and cause the left shift of the Mohr's circle (Cai et al. 2002), therefore, increasing the risk of failure.
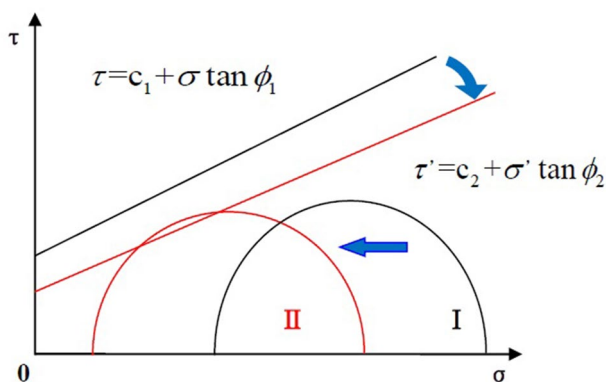

Fig. 11 Schematic diagram of the moving of Mohr–Coulomb circles and shear failure envelope before and after brine penetration

Cavern roof leakage analysis

In combination with the geological environment characteristics of the salt cavern, the upper part of the cavern is a thick and high permeable siltstone stratum. Generally, siltstone has a large range of permeability, which induces the different engineering measures for different type of siltstone (Wang et al. 2018). For instance, tight siltstone usually has extremely low permeability and hydra-fracturing is needed (Yuan et al. 2018). The physical characteristics analysis has revealed that the main composition of the roof layer includes gypsum, which would be partly dissolved in the water, leading to the softening of the roof layer and eventually causing the collapse of that roof under an underground high-pressure environment. The stability of the cavern would be greatly affected, and after the collapse of the roof, the cavern would directly be in contact with the upper Dainan siltstone layer, leading to the leakage of brine in the cavern. In this study, the Dainan siltstone has a permeability around 10^{-15} m^2, thus it has good water conductivity. But the leakage amount of brine needs qualitative analysis. Therefore, using Comsol software, the leakage evaluation of the cavern was simulated and qualitatively analyzed.

Model establishment

To simulate the actual situation of the salt cavern, a two-dimension seepage model was established as a cross profile, having an elliptical shape, with a maximum diameter of 100 m, a height of 80 m, and an exposing siltstone roof width of 40 m. The cavern is located in the salt rock formations and is buried at a depth of 1630–1720 m. There are gypsum layers in both the roof and the middle part, while the upper part contains the Dainan siltstone stratum and the lower part is made up of the mudstone layer.

At the beginning of the simulation, the roof gypsum mudstone had been peeled off, and the brine in the cavern was contacted with the Dainan siltstone. The initial brine pressure was set at 19 MPa, the initial pore water pressure in the surrounding rock was 0, and the density of brine was 1200 kg/m^3. The cavern is constantly replenished with brine water to maintain the internal pressure. Darcy's law physical

Table 5 Simulation parameters of the rock layer

Rock layer	Porosity (%)	Permeability (m^2)
Salt rock	1.0	1.0e−18
Interlayer	2.0	3.0e−17
Dainan siltstone	9.6	4.8e−15
Gypsum mudstone	9.5	1.5e−16

field (COMSOL Multiphysics User's guide 2014) was used, as shown in Eqs. (1) and (2). For seepage calculation, some related parameters of the rock layers in the simulation are shown in Table 5. After the failure of the roof, the brine penetration revolution of the Dainan siltstone layer within 1 year was studied.

$$\frac{\partial}{\partial t}\left(\varepsilon_p \rho\right) + \nabla \cdot (\rho u) = Q_m, \tag{1}$$

$$u = -\frac{k}{\mu}(\nabla p + \rho g \nabla D), \tag{2}$$

where ρ is fluid density, k is the permeability, μ is the viscosity of the fluid, p is fluid pressure, D is the position water head, Q_m is the source–sink term, and ε_p is the porosity.

Analysis of simulation results

As shown in Fig. 12, once the leakage begins, the brine seeps rapidly from the roof to the siltstone layer due to the great pressure difference. The penetration shape is radial, while the size of the arrow is directly proportional to the velocity of the seepage flow. Thus, the pore fluid pressure changes significantly in the Dainan siltstone layer. In the early stage, the pressure is rapidly increased, but the infiltration area exists only within a certain range. Then the decline rate gradually slows down and eventually stabilizes as the pores in the upper part of the roof are gradually saturated. The changes in pore pressure within 1 year are shown in Fig. 13.

The real-time variation curve of cavern leakage velocity is shown in Fig. 14. The leakage rate was the largest at the beginning of the simulation, and then it decreased rapidly and subsided a month later. The cumulative leakage of the cavern is given in Fig. 15, which was gradually increased, but the growth rate was slow, and after 1 year the cumulative leakage had reached the number of 3.14 million kilograms, which means the cumulative loss of the cavern in 1 year is 104,700 cubic meters. This amount is very large and can
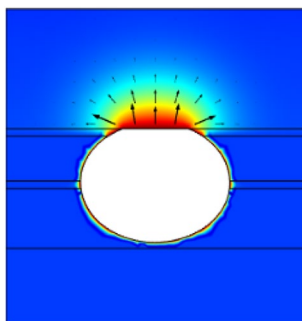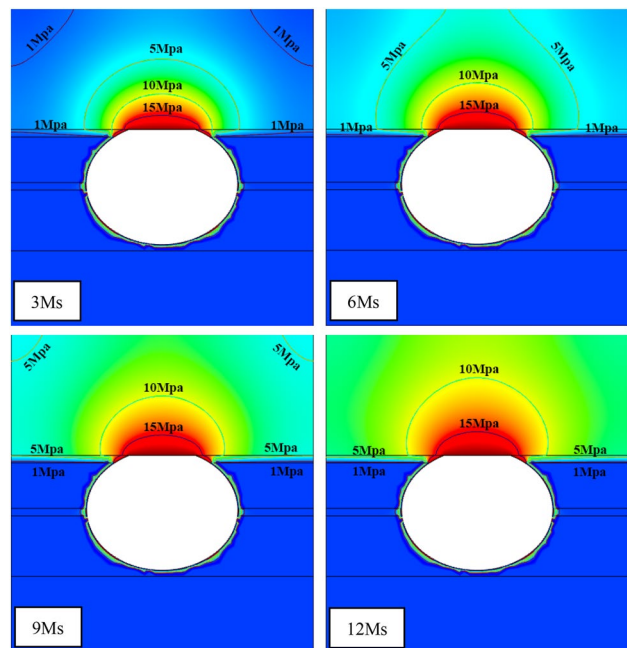

Fig. 13 Distribution of pore pressure in Dainan siltstone layer within 1 year

greatly affect the normal production capacity of the salt cavern. Also, we found the simulated brine leakage is much less than the field survey data, which is because the two-dimensional model equals only 1 m in thickness; therefore, the leakage area is much smaller than the actual one in the horizontal cavern at field.

Most of the time, salt caverns are regarded as ideal facilities owing remarkable tightness and stability as oil and gas storage. However, from this study, we can found that some salt caverns are also of poor stability and leakage probability. Then the application of them as energy storage is a risk. In fact, salt roof failure and even collapse are common geological disasters (Bérest 2017) all around the world. China has a lot of bedded salt rocks, if we hope to leach brine smoothly
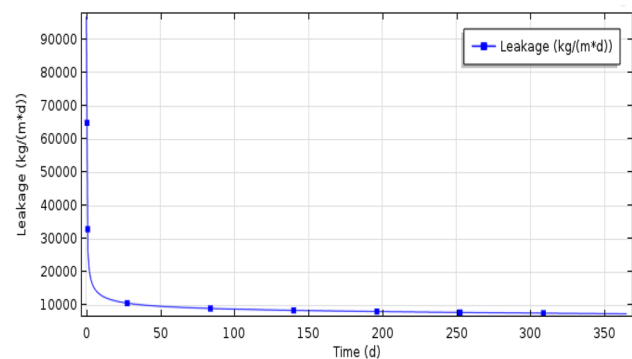

Fig. 12 Brine seepage velocity diagram in Dainan siltstone roof

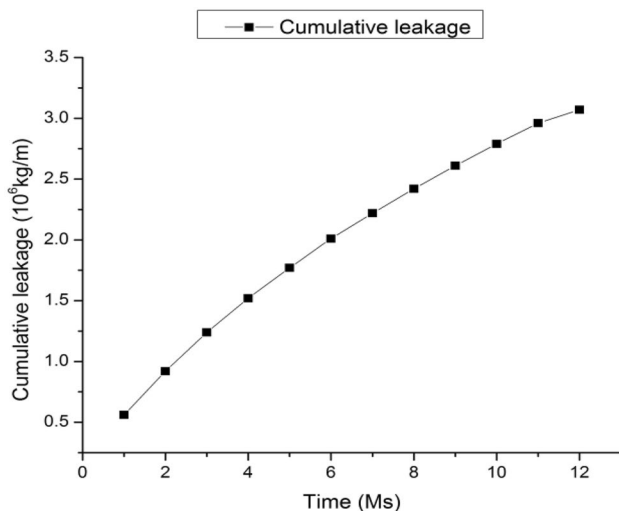**Fig. 14** The real-time variation curve of the brine leakage velocity

Fig. 15 The curve of accumulative brine leakage in the cavern

and even hope to use the caverns for later energy storage, the roof protection and risk of roof failure must be carefully assessed.

Conclusion and recommendations

Through the analysis of the geological exploration data of the leakage cavern, there are good reasons to think that the cavern roof is the most probable position of brine leakage. Therefore, a series of physical analysis experiments and numerical simulations were carried out on the core of roof strata. The analytical results showed that:

1. The main component of direct roof strata is gypsum mudstone, which can easily absorb water and expand under high brine pressure. If the upper solution of the cavern is not controlled effectively, the contact between the brine and this type of roof stratum will result in the softening and denudation of the roof strata, leading to the potential of brine loss and roof collapse.
2. After the collapse of first gypsum roof strata, the cavern was directly in contact with the upper Dainan siltstone, which showed a strong water adsorption and permeable properties the soaking experiment.
3. In the end, the brine was penetrating into the Dainan siltstone layer, which represents the leakage mechanism of the cavern. The roof strata permeable parameters of the leakage cavern are obtained by conducting the nuclear magnetic experiment.
4. Finally, by establishing a two-dimensional cavern seepage model and using Comsol software to calculate and obtain the variation process of brine loss in siltstone stratum, it was found that the leakage in the Dainan

siltstone roof was a large amount and the continuous production of cavern will be greatly impacted even interrupted.

It can then be concluded that if the upper solution of the cavern is effectively controlled, the collapse and leakage of the roof can be effectively prevented. Therefore, based on the existing experiments and production experience, it is suggested that, in the process of cavitation, the cavern technology of oil blanket should be used to control the dissolution rate. At the same time, the cavern should be provided with a suitable high-quality salt layer to protect the roof and to prevent the occurrence of similar accidents, especially for the caverns for later energy storage.

References

Bekendam F, Oldenziel CE, Paar W (2000) Subsidence potential of the hengelo brine field (Part I). Physico-Chemical deterioration and mechanical failure of salt cavern roof layers. In: Proceedings technical class and technical session, SMRI Fall Meeting, San Antonio. 15–16 October 2000. pp 103–117

Bérest P (2017) Cases, causes and classifications of craters above salt caverns. Int J Rock Mech Min Sci 100:318–319

Cai MF, He MC, Liu DY (2002) Rock Mechanics and Engineering[M]. Science Press, Beijing

Chen J, Jiang D, Ren S, Yang C (2016) Comparison of the characteristics of rock salt exposed to loading and unloading of confining pressures. Acta Geotech 11(1):221–230

Chen X, Li Y, Liu W et al (2018) Study on sealing failure of wellbore in bedded salt cavern gas storage[J]. Rock Mech Rock Eng 2018:1–14

Cosenza P, Ghoreychi M, Bazargan-Sabet B, de Marsily G (2009) In situ rock salt permeability measurement for long term safety assessment of storage. Int J Rock Mech Min Sci 36:509–526

Cuevas CDL (1997) Pore structure characterization in rock salt. Eng Geol 47(1–2):17–30

Djizanne H, Bérest P, Brouard B (2014) The mechanical stability of a salt cavern used for compressed air energy storage (CAES). Solution Mining Research Institute Spring 2014 Technical Conference San Antonio, Texas, USA, 5–6 May 2014

Houben ME, Hove AT, Peach CJ, Spiers CJ (2013) Crack healing in rock salt via diffusion in adsorbed aqueous films: microphysical modelling versus experiments. Phys Chem Earth 64:95–104

COMSOL Multiphysics User's guide (2014)

Johnson DO, Seni SJ (2001) Regulation of hydrocarbon storage operations in Texas. In: Proc SMRI Spring Meeting, Orlando, pp 111–120

Li Y, Shi X, Yang C, Qu D (2012) Several key problems about control of solution mining for oil/gas storage in deep salt mine. Chin J Rock Mech Eng 31(9):1785–1796 **(in Chinese)**

Liu W, Chen J, Jiang D, Shi X, Li Y, Daemen JJK et al (2016a) Tightness and suitability evaluation of abandoned salt caverns served as

hydrocarbon energies storage under adverse geological conditions (AGC). Appl Energy 178:703–720

Liu W, Muhammad N, Chen J, Spiers CJ, Peach CJ, Jiang D et al (2016b) Investigation on the permeability characteristics of bedded salt rocks and the tightness of natural gas caverns in such formations. J Nat Gas Sci Eng 35:468–482

Liu X, Yang X, Wang J, Li D, Li P, Yang Z (2016c) A dynamic dissolution model of rock salt under gravity for different flow rates. Arab J Geosci 9(3):1–8

Liu W, Jiang D, Chen J, Tang K, Wu F, Shi X (2018) Comprehensive feasibility study of two-well-horizontal caverns for natural gas storage in thinly-bedded salt rocks in China. Energy 143:1006–1019

Lux KH (2009) Design of salt caverns for the storage of natural gas, crude oil and compressed air: geomechanical aspects of construction, operation and abandonment. Geol Soc Lond Spec Publ 313:93–128

Ma H, Yang C, Li Y, Shi X, Liu J et al (2015) Stability evaluation of the underground gas storage in rock salts based on new partitions of the surrounding rock. Environ Earth Sci 73(11):6911–6925

Preece D, Foley J (1983) Finite element analysis of salt cavern employed in the strategic petroleum reserve. In: Proceedings of 6th International symposium on salt, 49–63

Preece D, Foley J (1984). Long-term performance predictions for SPR salt caverns. SAND83-2343, Sandia National Laboratories, Albuquerque, NM

Shi X, Li Y, Yang C et al (2009) Experimental study on the effect of brine immersion on the tensile strength of argillaceous interlayer. Chin J Rock Mech Eng 28(11):2301–2308

Shi X, Li Y, Yang C, Xu Y, Ma H, Wei L et al (2015) Influences of filling abandoned salt caverns with alkali wastes on surface subsidence. Environ Earth Sci 73(11):6939–6950

Shi X, Liu W, Chen J, Jiang D, Wu F, Zhang J et al (2018) Softening model for failure analysis of insoluble interlayers during salt cavern leaching for natural gas storage. Acta Geotech 13(4):801–816

Wang J, Zhang S, Zhao B, Liu X, Liu J, Lai J (2018) A study on the mechanical behavior and statistical damage constitutive model of sandstone. Arab J Sci Eng 43(10):5179–5192

Wu F, Chen J, Zou Q (2018) A nonlinear creep damage model for salt rock. Int J Frac Eng Int J Damage Mech. https://doi.org/10.1177/1056789518792649

Xing W, Zhao J, Hou Z et al (2015) Horizontal natural gas caverns in thin-bedded rock salt formations. Environ Earth Sci 73(11):6973–6985

Yang C, Jing W, Daemen JJK, Zhang G (2013) Analysis of major risks associated with hydrocarbon storage caverns in bedded salt rock. Reliab Eng Syst Safe 113(1):94–111

Yang C, Wang T, Li Y, Yang H, Li J, Qu D et al (2015) Feasibility analysis of using abandoned salt caverns for large-scale underground energy storage in China. App Energy 137:467–481

Yang C, Wang T, Qu D, Ma H, Li Y, Shi X et al (2016) Feasibility analysis of using horizontal caverns for underground gas storage: a case study of Yunying salt district. J Nat Gas Sci Eng 36:252–266

Yuan W, Wang W, Su X, Li Li Jia, Zong Li, Wen L et al (2018) Numerical study of the impact mechanism of decoupling charge on blasting-enhanced permeability in low-permeability sandstones. Int J Rock Mech & Min Sci 2018(106):300–310

Zhang G, Li Y, Yang C, Daemen JJK (2014) Stability and tightness evaluation of bedded rock salt formations for underground gas/oil storage. Acta Geotech 9(9):161–179

Zhang G, Li Y, Daemen JJK, Yang C, Wu Y (2015) Geotechnical feasibility analysis of compressed air energy storage (CAES) in bedded salt formations: a case study in Huai'an City, China. Rock Mech Rock Eng 48(5):2111–2127

Zhang N, Shi X, Wang T, Yang C, Liu W (2017) Stability and availability evaluation of underground strategic petroleum reserve (SPR) caverns in bedded rock salt of Jintan, China. Energy 134:504–514